CHEMCATCHEM COMMUNICATIONS

ChemPubSoc Europe

DOI: 10.1002/cctc.201402647

Investigation of the Kinetics of a Surface Photocatalytic Reaction in Two Dimensions with Surface-enhanced Raman Scattering

Evelien M. van Schrojenstein Lantman,[a] Onno L. J. Gijzeman,[b] Arjan J. G. Mank,[c] and Bert M. Weckhuysen*[a]

Heterogeneous catalysis is a surface phenomenon. Yet, though the catalysis itself takes place on surfaces, the reactants and products rapidly take the form of another physical state, as either a liquid or a gas. Catalytic reactions within a self-assembled monolayer are confined within two dimensions, as the molecules involved do not leave the surface. Surface-enhanced Raman spectroscopy is an ideal technique to probe these self-assembled monolayers as it gives molecular information in a measured volume limited to the surface. We show how surface-enhanced Raman spectroscopy can be used to determine the reaction kinetics of a two-dimensional reaction. As a proof of principle, we study the photocatalytic reduction of *p*-nitrothiophenol. A study of the reaction rate and dilution effects leads to the conclusion that a dimerization must take place as one of the reaction steps.

The interaction between reactants at catalytic surfaces has been the study of many years,[1] and novel techniques are used readily to gain more insight into chemical processes as they happen.[2] Surface-enhanced Raman spectroscopy (SERS) is gaining increasing popularity in this field as a powerful characterization tool.[3] Typically, silver or gold nanostructured surfaces are used to enhance Raman spectra of molecules, with a sensitivity that reaches single-molecule levels.[4] This high sensitivity also makes it applicable in, for example, forensic trace detection[5] or biomolecular assays.[6] As SERS is highly confined to the metal surface, it allows for the selective study of the molecules in close proximity to the surface. This high spatial confinement makes SERS ideal to follow reactions on a catalytic surface. The use of self-assembled monolayers (SAMs) allows us to create a single reactant layer at this catalytic surface.

Common characterization techniques for SAMs include grazing incidence angle IR spectroscopy, X-ray photoelectron spectroscopy, scanning tunneling microscopy, and atomic force microscopy.[7] SERS gives more localized, molecular information than grazing angle IR spectroscopy, whereas in the future, the combination with atomic force microscopy in tip-enhanced Raman spectroscopy is expected to go to the extreme of combining both molecular information and nanoscale resolution.[8] The few reactions in SAMs reported to date are observed by using atomic force microscopy,[9] scanning tunneling microscopy,[10] or SERS,[10b,11] and are nearly all photoreactions, for example, UV-induced photoisomerizations,[10a] or dimerizations, either within a SAM of the pure reactant,[11b] or in a diluted form.[10b]

A typical heterogeneous catalytic reaction at a surface involves three separate steps, as shown in Figure 1a, whereas

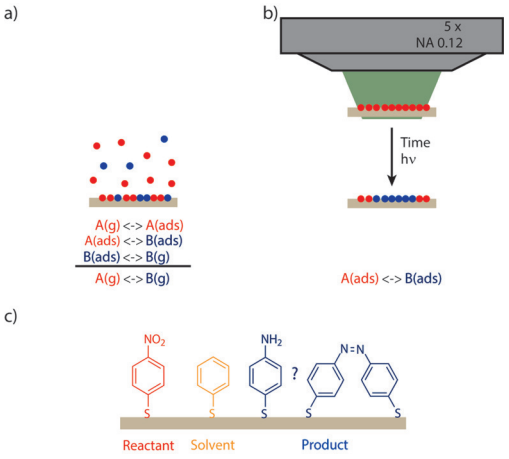

Figure 1. a) Reaction steps in a typical heterogeneous catalytic reaction from A(g) to B(g) involve adsorption of reactants A onto the catalytic surface, a surface-reaction yielding a reaction product B, and subsequent desorption of the reaction products into the gas environment. b) A photocatalytic surface reaction is studied. Novel with respect to part a is that only the surface-reaction is monitored, as a function of irradiation at $\lambda = 532$ nm (5× objective, NA 0.12). c) The reaction under study is the photoreduction of pNTP to either *p*-aminothiophenol or DMAB. For dilution experiments, thiophenol is used as the 2D equivalent to a solvent.

[a] *E. M. van Schrojenstein Lantman, Prof. Dr. B. M. Weckhuysen*
Inorganic Chemistry and Catalysis
Debye Institute for Nanomaterials Science
Utrecht University
Universiteitsweg 99, 3584 CG Utrecht (The Netherlands)
E-mail: b.m.weckhuysen@uu.nl

[b] *Dr. O. L. J. Gijzeman*
Condensed Matter and Interfaces
Debye Institute for Nanomaterials Science
Utrecht University
Princetonplein 1, 3584 CC Utrecht (The Netherlands)

[c] *Dr. A. J. G. Mank*
Materials Analysis—MiPlaza
Philips Innovation Services
High Tech Campus 11, 5656 AE Eindhoven (The Netherlands)

Supporting information for this article is available on the WWW under http://dx.doi.org/10.1002/cctc.201402647.

a reaction within a SAM follows 2D reaction kinetics on the catalyst surface (Figure 1b). One of the most described reactions in a SAM is the photocatalytic reduction of *p*-nitrothiophenol (pNTP). A large discussion point is the interpretation of the reaction product SERS spectrum, which could indicate either *p*-aminothiophenol (pATP)[12] or *p,p'*-dimercaptoazobenzene (DMAB)[13] (see also Figure 1c). The challenge in the identification of the reaction product through other characterization techniques is twofold: an extremely low number of molecules are converted during the reaction and these few molecules are chemically bound to the surface. The latest developments indicate that the oxidation of pATP to DMAB is possible through a simultaneous plasmonic activation of oxygen.[14] This is further supported by a thorough theoretical study into the reaction pathway.[15] Others are still convinced that the reduction product of pNTP is pATP, based on a deviation of the Raman spectrum of neat pATP owing to chemical enhancement.[16]

SERS has previously been used to monitor reaction kinetics of various reactions.[17] With the right morphology of the SERS substrate, quantitative information can be obtained.[18] pNTP especially has been studied for its reduction reaction through, for example, electrochemical,[19] chemical,[20] or photochemical reduction.[8d,16b,19h,20d,21] All these reactions take place on the surface of either an electrode or nanoparticles, with possible exchange mechanisms into the solution in which the substrate is immersed. The photocatalytic reaction studied here is unique because the full reaction takes place within the two dimensions of the self-assembled monolayer. This has previously been examined, but not in detail, let alone with regards to the detailed mechanism of the reaction.

Time-resolved SERS spectra of the photocatalytic reaction provide the information to investigate these 2D reaction kinetics. We also show the dilution of the reactant on the surface with a similar but inert thiol. This dilution approach is the 2D equivalent of a solvent and will provide the ultimate evidence for whether a dimerization process is involved in the reaction mechanism of the photocatalytic reduction of pNTP.

Silver island films are used as the SERS substrate. These are rough on the nanoscale (Figure S1a) but homogeneous in morphology on the scale of the measurements described here. The SERS enhancement (Figure S1b) effect over this substrate shows a homogeneous distribution, as does the maximum catalytic conversion of the same area (Figure S1c). Small deviations between positions owe likely to noise in the spectra. In other words, the SERS intensity of this substrate is highly reproducible. Further precautions include the use of a large focal area, by using a 5× objective [numerical aperture (NA) 0.12], and low laser power. This results in a stable signal in time, without the characteristic spectral fluctuations related to single hotspot measurements.

With green laser excitation, pNTP will be reduced if it is adsorbed onto a SERS-active substrate,[21e] as illustrated in Figure 2a. All experiments were performed by using a low NA objective, to limit the effect of any local heterogeneities in the catalytic activity. The two characteristic Raman peaks for tracking the reaction are 1335 cm^{-1} (reactant pNTP, asymmetric NO_2 stretch)[22] and 1440 cm^{-1} (product, assigned to pATP as a b_2 mode[23] or to DMAB as a N=N stretch).[13a] Tracking both peak areas as a function of time gives an idea of the surface concentration of both species (Figure 2b). The concentration of pNTP decays over time, while the product is formed synchronously. The postulated multistep reaction mechanism[24] is expected to have a single rate-determining step. Therefore, we approximate the reaction to have one step and identify the order of reaction of this rate-limiting step.

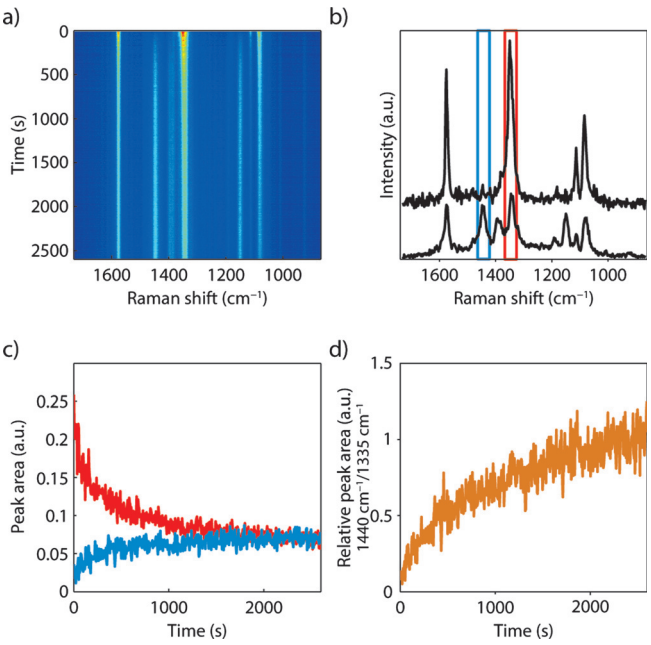

Figure 2. a) Time-dependent SERS measurements at $\lambda = 532$ nm from a pNTP-coated silver island film; each horizontal line represents a spectrum (blue–red: low–high signal intensity). b) The first (top) and last (bottom) spectrum of part a. The colored bands depict peak integration area for quantification of pNTP ($\tilde{\nu} = 1293$–1373 cm^{-1} and product ($\tilde{\nu} = 1412$–1473 cm^{-1}) over time. c) Time traces for pNTP (——) and product (——) taken from the peak areas marked in part b. d) Relative peak area as function of time. Spectra were taken with 5 s integration time at 6×10^3 $W\,cm^{-2}$.

The ratio of product to reactant (Figure 2c) flattens off at a specific value rather than continuing to infinity. The maximum conversion is dependent on the exact reaction conditions. For example, a much higher conversion is shown in Figure 3. In terms of reaction rate, a factor must be present to set a limit to complete conversion of the full SAM through the forward reaction. Possible contributions are a backward reaction or diffusion processes within the SAM. To test for these contributions to the reaction rate, sample illumination was blocked for significant periods of time. The results of this experiment are shown in Figure 3. It is clear that these dark periods do not have any effect on the peak area of either reactant or product (Figure 3).

We note that these results indicate that no full conversion is achieved (Figure 2d) and no significant contributions to the reaction rate are found, other than the forward reaction (Figure 3). Manufacturing variations in the plasmonic nature of the silver substrate will contribute to the total SERS enhancement of a substrate. However, only variations in the catalytic

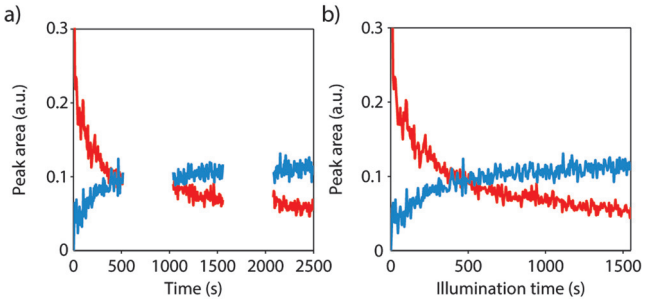

Figure 3. a) SERS peak areas for pNTP and product over time, with intermittent illumination; the Raman excitation laser was blocked from the sample between 500 and 1000 s and 1500 and 2000 s. b) The same data as shown in part a but without the dark periods. Spectra were taken with 5 s integration time at 6×10^3 W cm^{-2}.

activity of the silver surface can contribute to a variation in the maximum conversion. The most realistic explanation is therefore a contribution to the SERS signal from a photocatalytically inert part of the silver surface. This variation in photocatalytic activity must therefore also be taken into account when describing the reaction rate through the (surface-enhanced) Raman intensity.

For the surface dynamics, a full surface coverage is assumed at all times during the reaction. As described earlier, we have simplified the reaction to a one-step reaction and therefore assume only reactant and product molecules to be present at the surface. The derivation of the first and second-order reaction kinetics can be found in the Supporting Information. In short, the conversion of reactant A to product B is described in terms of the reaction constant k. The surface coverage of reactant, here denoted A, is described as the total number of surface sites in the measurement area ($N_{catalytic}+N_{inert}$) multiplied by the relevant fraction of sites occupied by reactant A (θ_A). The original surface coverage is set to $\theta_{A,0}$. The correction from surface coverage to Raman intensity (I) for the measured vibrations is made through Raman cross sections σ_A and σ_B.

For a first-order reaction, this yields Equation (1) and (2):

$$I_A = \sigma_A N_{catalytic} \theta_{A,0} e^{-kt} + \sigma_A N_{inert} \theta_{A,0} \quad (1)$$

$$I_B = \sigma_B N_{catalytic} \theta_{A,0} (1-e^{-kt}) \quad (2)$$

For the case of a second-order reaction or dimerization, Equation (3) and (4) describe the second-order reaction kinetics:

$$I_A = \sigma_A N_{catalytic} \theta_{A,0} \frac{1}{k\theta_{A,0} t + 1} + \sigma_A N_{inert} \theta_{A,0} \quad (3)$$

$$I_B = \sigma_B N_{catalytic} \theta_{A,0} \left(1 - \frac{1}{k\theta_{A,0} t + 1}\right) \quad (4)$$

Application of Equations (1)–(4) enables a quantitative description of the reaction (see Table 1). The values presented are representative for similar experiments (see Figure S2), though a distribution in both reaction rates and the fraction of catalytically active sites has been observed. Despite the low magnification objective used for these experiments, this distribution is probably still caused by variations in the SERS activity (e.g., oxidation degree, roughness) of the silver island films. The fraction of catalytically active surface sites $\sigma_A N_{catalytic}\theta_{A,0}/(\sigma_A N_{catalytic}\theta_{A,0}+\sigma_A N_{inert}\theta_{A,0})$ is roughly two thirds of the total SERS intensity. This could have a large effect at low laser power density. A high laser power density (see Figure S3) results in full conversion.

Table 1. Fit parameters of Equations (1)–(4) for the results shown in Figure 2b after use of a Savitzky–Golay filter. Fits can be viewed in Figure S2 and Table S1.

	First order	Second order
$\sigma_A N_{catalytic}\theta_{A,0}$	0.129(±2%)	0.1658(±2%)
$\sigma_B N_{catalytic}\theta_{A,0}$	0.0691(±1%)	0.0752(±1%)
k [s^{-1}]	0.00319(±3%)	–
$k\theta_{A,0}$ [s^{-1}]	–	0.00584(±4%)
$\sigma_A N_{inert}\theta_{A,0}$	0.0782(±1%)	0.0632(±1%)
R^2	0.90	0.95

Based on the R^2 values for the various fits in Table 1, the reaction rate is better described with second-order reaction kinetics. In addition, fit residuals (see Figure S2) also show a better fit for second-order reaction kinetics, especially at the start of the reaction. It is therefore likely that the rate-limiting step of the reaction is of second order. The reaction constant has an order of magnitude of 1×10^{-3} s^{-1}, similar to a previously reported value.[20e] The relative Raman cross section ($\sigma_B N_{catalytic}\theta_{A,0}/\sigma_A N_{catalytic}\theta_{A,0}$) indicates a similar Raman cross section for the reaction product as for the reactant. These results are reproducible under these reaction conditions, as also shown in Figure S4 and Tables S2 and S3.

Besides describing reactions quantitatively, reaction kinetics in combination with SERS can also be employed to examine other relations. In the case of discrimination between first and second-order reactions, it is insightful to examine the reaction rate of diluted SAMs. In this particular reaction, we have studied a mixed SAM under exactly the same reaction conditions as those described in Figure 2. The vast difference is in the consistency of the SAM: roughly 1% of the SAM consists of pNTP, the rest is thiophenol, which acts as a 2D "solvent". The reaction rate of a pure first-order reaction would be independent of the initial reactant concentration [Eq. (1)], whereas a hundredfold dilution is expected to result in a similar decrease in reaction rate [Eq. (3)]. This is exactly the case, as shown in Figure 4. The small quantity of pNTP in the SAM still reveals the SERS signal. The reduced intensity of the reactant peak is likely to owe to some degree of degradation or reorganization of the SERS substrate. This can negatively influence the reaction rate if it is of second (or higher) order, resulting in a lower measured reaction rate. In the case of first-order reaction kinetics, bleaching will not affect the reaction rate.

Here, no product-formation whatsoever is observed on this timescale, as none of the characteristic product peaks are visible at the end of the measurement, in contrary to the measurements shown in Figure 2. This provides the final proof that the ambient photoreduction of pNTP involves a dimerization

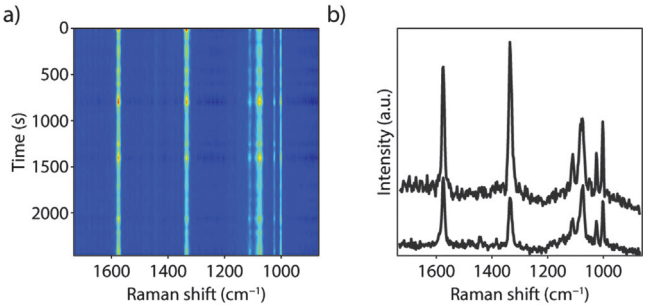

Figure 4. a) Time-dependent SERS measurements (blue–red: low–high signal intensity) of the reaction over time on a sample with a 1% surface coverage of pNTP. b) The first (top) and last (bottom) spectrum of the time series shown in part a. Spectra were taken at 50 s integration time.

step. The formation of DMAB is at least the rate-limiting step and DMAB a reaction intermediate, if not simply the reaction product.

In conclusion, we have described the photocatalytic reduction of *p*-nitrothiophenol with a novel 2D approach in terms of reaction kinetics by means of surface-enhanced Raman spectroscopy (SERS). By following the characteristic Raman peaks, $\tilde{\nu} = 1335\ cm^{-1}$ for *p*-nitrothiophenol and $1440\ cm^{-1}$ for the product, we have shown in two distinctly different ways that this photocatalytic reduction at the very least involves a dimerization reaction. The rate-limiting reaction of pure self-assembled monolayers of *p*-nitrothiophenol of silver SERS substrates was shown to be of the second order and is only influenced by the forward reaction. Complete conversion was held back by a contribution of the SERS signal from a non-catalytically active SERS surface. The most compelling evidence for a dimerization was obtained through incorporation of an inert thiol into the self-assembled monolayers of *p*-nitrothiophenol. Thiophenol was thus used as the 2D equivalent of a solvent. The reaction rate was slowed down extremely by this dilution effect, up to the point that no reaction was observed under the standard reaction conditions—hence proving that a second-order reaction was involved.

Chemistry in 2D space, occurring in a confined space, appears a rather abstract theme. However, it is in fact applicable to any field dealing with interfacial chemistry, for example, cellular membranes, biomedical material interfaces, molecular electronics, and solar fuel generation. Reactions or interactions within these interfaces are all limited to the 2D space they occupy. Therefore, the developed SERS approach is generally applicable to other instances of surface chemistry.

Experimental Section

Silver island films were prepared by vacuum deposition of 7 nm silver onto glass coverslips. Directly before use, films were annealed for 1 min at 300 °C under argon. The SERS substrates were immediately immersed in fresh 2 mM ethanolic thiol solutions for 15–18 h. To alter the pNTP (Fluka, technical grade) surface concentration, the ratio between pNTP and thiophenol (Merck, for synthesis) was adjusted to keep the total thiol concentration constant. X-ray photoelectron spectroscopy measurements indicated no large deviation in thiol ratio once adsorbed onto the silver island film.

SERS spectra were measured through a 5× objective (NA 0.12) at 532 nm excitation with a power density of $6 \times 10^3\ W\,cm^{-2}$ by using a Renishaw InVia Raman microscope. The microscope registered the time at which a spectrum recording finished. The preceding measurement time was taken into account when fitting the data.

Data processing was done with Matlab 2013a and the baseline-corrected peak integration performed by using trapezoidal numerical integration. Normalization of the total SERS intensity was performed on the basis of the total SERS intensity between 1020 and $1625\ cm^{-1}$. A zero-order Savitzky–Golay filter of 7 pixels was used to smooth the time-dependent peak areas. The NonlinearModelFitting function in Mathematica 9.0 was used for fitting both the reactant and product smoothed time traces simultaneously. The sum of residuals and squares was calculated separately for both reactant and product, then added, to calculate R^2.

Acknowledgements

This work is supported by the Netherlands Research School Combination-Catalysis (NRSC-C), a European Research Council (ERC) Advanced Grant (no. 321140), and NanoNextNL, a micro- and nanotechnology consortium of the Government of the Netherlands and 130 partners.

Keywords: heterogeneous catalysis · Raman spectroscopy · reaction kinetics · self-assembly · surface-enhanced Raman scattering

[1] a) G. A. Somorjai, Y. Li, *Introduction to Surface Chemistry and Catalysis, 2nd ed.*, Wiley-VCH, Weinheim, **2010**; b) G. A. Somorjai, H. Frei, J. Y. Park, *J. Am. Chem. Soc.* **2009**, *131*, 16589 – 16605; c) *Handbook of Heterogeneous Catalysis, 2nd ed.* (Eds.: G. Ertl, H. Knözinger, F. Schüth, J. Weitkamp), Wiley-VCH, Weinheim, **2008**; d) G. Ertl, *Angew. Chem. Int. Ed.* **2008**, *47*, 3524 – 3535; *Angew. Chem.* **2008**, *120*, 3578 – 3590; e) J. Hagen, *Industrial Catalysis: A Practical Approach*, Wiley-VCH, Weinheim, **1999**.

[2] a) I. L. C. Buurmans, B. M. Weckhuysen, *Nat. Chem.* **2012**, *4*, 873 – 886; b) M. A. Bañares, *Adv. Mater.* **2011**, *23*, 5293 – 5301; c) F. Tao, M. Salmeron, *Science* **2011**, *331*, 171 – 173; d) B. M. Weckhuysen, *Chem. Soc. Rev.* **2010**, *39*, 4557 – 4559; e) *In situ Spectroscopy of Catalysts* (Ed.: B. M. Weckhuysen), American Scientific Publishers, Stevenson Ranch, **2004**; f) H. Topsøe, *J. Catal.* **2003**, *216*, 155 – 164.

[3] H. Kim, K. M. Kosuda, R. P. Van Duyne, P. C. Stair, *Chem. Soc. Rev.* **2010**, *39*, 4820 – 4844.

[4] E. C. Le Ru, P. G. Etchegoin, *Annu. Rev. Phys. Chem.* **2012**, *63*, 65 – 87.

[5] F. Inscore, C. Shende, A. Sengupta, H. Huang, S. Farquharson, *Appl. Spectrosc.* **2011**, *65*, 1004 – 1008.

[6] M. M. Harper, K. S. McKeating, K. Faulds, *Phys. Chem. Chem. Phys.* **2013**, *15*, 5312 – 5328.

[7] C. Vericat, M. E. Vela, G. Benitez, P. Carro, R. C. Salvarezza, *Chem. Soc. Rev.* **2010**, *39*, 1805 – 1834.

[8] a) Z. Zhang, S. Sheng, H. Zheng, H. Xu, M. Sun, *Nanoscale* **2014**, *6*, 4903 – 4908; b) R. Zhang, Y. Zhang, Z. C. Dong, S. Jiang, C. Zhang, L. G. Chen, L. Zhang, Y. Liao, J. Aizpurua, Y. Luo, J. L. Yang, J. G. Hou, *Nature* **2013**, *498*, 82 – 86; c) M. Sun, Z. Zhang, Z. H. Kim, H. Zheng, H. Xu, *Chem. Eur. J.* **2013**, *19*, 14958 – 14962; d) M. Sun, Z. Zhang, H. Zheng, H. Xu, *Sci. Rep.* **2012**, *2*, 647; e) E. M. van Schrojenstein Lantman, T. Deckert-Gaudig, A. J. G. Mank, V. Deckert, B. M. Weckhuysen, *Nat. Nanotechnol.* **2012**, *7*, 583 – 586; f) K. F. Domke, B. Pettinger, *ChemPhysChem* **2010**, *11*, 1365 – 1373.

[9] a) W. T. Müller, D. L. Klein, T. Lee, J. Clarke, P. L. McEuen, P. G. Schultz, *Science* **1995**, *268*, 272 – 273; b) C. Blackledge, D. A. Engebretson, J. D. McDonald, *Langmuir* **2000**, *16*, 8317 – 8323.

[10] a) B. K. Pathem, Y. B. Zhen, S. Morton, M. A. X. Petersen, Y. Zhao, C.-H. Chung, Y. Yang, L. Jensen, M. B. N. Nielsen, P. S. Weiss, *Nano Lett.* **2013**, *13*, 337 – 343; b) M. Kim, J. N. Hohman, Y. Cao, K. N. Houk, H. Ma, A. K.-Y. Jen, P. S. Weiss, *Science* **2011**, *331*, 1312 – 1315.

[11] a) Y. B. Zheng, J. L. Payton, C.-H. Chung, R. Liu, S. Cheunkar, B. K. Pathem, Y. Yang, L. Jensen, P. S. Weiss, *Nano Lett.* **2011**, *11*, 3447 – 3452; b) Y. B. Zheng, J. L. Payton, T.-B. Song, B. K. Pathem, Y. Zhao, H. Ma, Y. Yang, L. Jensen, A. K.-Y. Jen, P. S. Weiss, *Nano Lett.* **2012**, *12*, 5362 – 5368.

[12] a) K. Kim, J. K. Yoon, H. B. Lee, D. Shin, K. S. Shin, *Langmuir* **2011**, *27*, 4526 – 4531; b) K. Kim, H. B. Lee, D. Shin, H. Ryoo, J. W. Lee, K. S. Shin, *J. Raman Spectrosc.* **2011**, *42*, 2112 – 2118; c) K. Kim, K. L. Kim, J.-Y. Choi, D. Shin, K. S. Shin, *Phys. Chem. Chem. Phys.* **2011**, *13*, 15603 – 15609; d) K. Kim, D. Shin, K. L. Kim, K. S. Shin, *Phys. Chem. Chem. Phys.* **2012**, *14*, 4095 – 4100; e) K. Kim, D. Sin, J.-Y. Choi, K. L. Kim, K. S. Shin, *J. Phys. Chem. C* **2011**, *115*, 24960 – 24966; f) K. Kim, K. L. Kim, D. Shin, J.-Y. Choi, K. S. Shin, *J. Phys. Chem. C* **2012**, *116*, 4774 – 4779; g) K. Kim, K. L. Kim, H. B. Lee, K. S. Shin, *J. Phys. Chem. C* **2012**, *116*, 11635 – 11642; h) K. Kim, K. L. Kim, K. S. Shin, *Langmuir* **2013**, *29*, 183 – 190; i) K. Kim, K. L. Kim, K. S. Shin, *J. Phys. Chem. C* **2013**, *117*, 5975 – 5981.

[13] a) Y. F. Huang, H.-P. Zhu, G.-K. Liu, D.-Y. Wu, B. Ren, Z.-Q. Tian, *J. Am. Chem. Soc.* **2010**, *132*, 9244 – 9246; b) Y. Huang, Y. Fang, Z. Yang, M. Sun, *J. Phys. Chem. C* **2010**, *114*, 18263 – 18269; c) M. Sun, Y. Huang, L. Xia, X. Chen, H. Xu, *J. Phys. Chem. C* **2011**, *115*, 9629 – 9636; d) Y.-F. Huang, D.-Ye. Wu, H.-P. Zhu, L.-B. Zhao, G.-K. Liu, B. Ren, Z.-Q. Tian, *Phys. Chem. Chem. Phys.* **2012**, *14*, 8485 – 8497; e) V. Canpean, S. Astilean, *Spectrochim. Acta Part A* **2012**, *96*, 862 – 867.

[14] a) Y.-F. Huang, M. Zhang, L.-B. Zhao, J.-M. Feng, D.-Y. Wu, B. Ren, Z.-Q. Tian, *Angew. Chem. Int. Ed.* **2014**, *53*, 2353 – 2357; *Angew. Chem.* **2014**, *126*, 2385 – 2389; b) P. Xu, L. Kang, N. H. Mack, K. S. Schanze, X. Han, H.-L. Wang, *Sci. Rep.* **2013**, *3*, 2997.

[15] L.-B. Zhao, M. Zang, Y.-F. Huang, C. T. Williams, D-Y. Wu, B. Ren, Z.-Q. Tian, *J. Phys. Chem. Lett.* **2014**, *5*, 1259 – 1266.

[16] a) K. Kim, J.-Y. Choi, K. S. Shin, *J. Phys. Chem. C* **2013**, *117*, 11421 – 11427; b) K. S. Shin, Y. K. Cho, K. Kim, *Vib. Spectrosc.* **2014**, *70*, 120 – 124.

[17] a) B. D. Moore, L. Stevenson, A. Watt, S. Flitsch, N. J. Turner, C. Cassidy, D. Graham, *Nat. Biotechnol.* **2004**, *22*, 1133 – 1138; b) H. Wackerbarth, U. Klar, W. Günther, P. Hildebrandt, *Appl. Spectrosc.* **1999**, *53*, 283 – 291; c) K. N. Heck, B. G. Janesk, G. E. Scuseria, N. J. Halas, M. S. Wong, *J. Am. Chem. Soc.* **2008**, *130*, 16592 – 16600.

[18] S. Kasera, F. Biedermann, J. J. Baumberg, O. A. Scherman, S. Mahajan, *Nano Lett.* **2012**, *12*, 5924 – 5928.

[19] a) N. Matsuda, K. Yoshii, K.-I. Ataka, M. Osawa, T. Matsue, I. Uchida, *Chem. Lett.* **1992**, 1385 – 1388; b) N. Matsuda, T. Sawaguchi, M. Osawa, I. Uchida, *Chem. Lett.* **1995**, 145 – 146; c) M. Futamata, *J. Phys. Chem.* **1995**, *99*, 11901 – 11908; d) T. Zhu, H. Z. Yu, Y. C. Wang, Z. F. Liu, *Mol. Cryst. Liq. Cryst. Sci. Technol. Sect. A* **1999**, *337*, 241 – 244; e) J. U. Nielsen, M. J. Explandiu, D. M. Kolb, *Langmuir* **2001**, *17*, 3454 – 3459; f) M. Futamata, C. Nishihara, N. Goutev, *Surf. Sci.* **2002**, *514*, 241 – 248; g) S. Schwamborn, L. Stoica, S. Neugebauer, T. Reda, H.-L. Schmidt, W. Schuhmann, *ChemPhysChem* **2009**, *10*, 1066 – 1070; h) X. Zhang, P. Wang, Z. Zhang, Y. Fang, M. Sun, *Sci. Rep.* **2014**, *4*, 5407.

[20] a) W. Xie, C. Herrmann, K. Kömpe, M. Haase, S. Schlücker, *J. Am. Chem. Soc.* **2011**, *133*, 19302 – 19305; b) V. Joseph, C. Engelbrekt„ J. Zhang, U. Gernert, J. Ulstrup, J. Kneipp, *Angew. Chem. Int. Ed.* **2012**, *51*, 7592 – 7596; *Angew. Chem.* **2012**, *124*, 7712 – 7716; c) W. Xie, B. Walkenfort, S. Schlücker, *J. Am. Chem. Soc.* **2013**, *135*, 1657 – 1660; d) X. Ren, E. Tan, X. Lang, T.-T. You, L. Jiang, H. Zhang, P. Yin, L. Guo, *Phys. Chem. Chem. Phys.* **2013**, *15*, 14196 – 14201; e) J. Huang, Y. Zhu, M. Lin, Q. Wang, L. Zhao, Y. Yang, K. X. Yao, Y. Han, *J. Am. Chem. Soc.* **2013**, *135*, 8552 – 8561; f) R. Liu, J.-F. Liu, Z.-M. Zhang, L.-Q. Zhang, J.-F. Sun, M. Sun, G.-N. Jiang, *J. Phys. Chem. Lett.* **2014**, *5*, 969 – 975.

[21] a) X. M. Yang, D. A. Tryk, K. Ajito, K. Hashimoto, A. Fujishima, *Langmuir* **1996**, *12*, 5525 – 5527; b) K. Kim, I. Lee, S. J. Lee, *Chem. Phys. Lett.* **2003**, *377*, 201 – 204; c) S. J. Lee, K. Kim, *Chem. Phys. Lett.* **2003**, *378*, 122 – 127; d) K. S. Shin, C. S. Park, W. Kang, K. Kim, *Chem. Lett.* **2008**, *37*, 180 – 181; e) K. Kim, Y. M. Lee, H. B. Lee, Y. Park, T. Y. Bae, Y. M. Jung, C. H. Choi, K. S. Shin, *J. Raman Spectrosc.* **2010**, *22*, 187 – 192; f) B. Dong, Y. Fang, X. Chen, H. Xu, M. Sun, *Langmuir* **2011**, *27*, 10677 – 10682; g) K. Kim, K. L. Kim, K. S. Shin, *J. Phys. Chem. C* **2011**, *115*, 23374 – 23380; h) L. Kang, P. Xu, B. Zhang, H. Tsai, X. Han, H.-L. Wang, *Chem. Commun.* **2013**, *49*, 3389 – 3391; i) T. You, L. Jiang, P. Yin, Y. Shang, D. Zhang, L. Guo, S. Yang, *J. Raman Spectrosc.* **2014**, *45*, 7 – 14.

[22] B. O. Skadtchenko, R. Aroca, *Spectrochim. Acta Part A* **2001**, *57*, 1009 – 1016.

[23] M. Osawa, N. Matsuda, K. Yoshii, I. Uchida, *J. Phys. Chem.* **1994**, *98*, 12702 – 12707.

[24] S. Sun, R. L. Birke, J. R. Lombardi, K. P. Leung, A. Z. Genack, *J. Phys. Chem.* **1988**, *92*, 5965 – 5972.

Received: August 15, 2014
Revised: September 23, 2014
Published online on October 29, 2014